Rate Parameters for Coupled Rotation-Vibration-Dissociation Phenomena in H_2

Surendra P. Sharma* and David W. Schwenke†
NASA Ames Research Center, Moffett Field, California 94035

A theoretical study of the effects of molecular rotation on coupled vibration-dissociation phenomena for H_2, undergoing a nonequilibrium relaxation in a heating and cooling environment, is reported. The rate coefficients for the collisional bound-bound and bound-free transitions have been calculated using a quasi-classical trajectory method. These state-to-state transition rates were fed into the master equation, which was numerically solved to determine the rotational and vibrational population densities as well as the bulk thermodynamic properties. Our results show that a) the vibrational transition rates of H_2 increase monotonically with the vibrational levels, faster than the Landau-Teller model, b) the rotation of the molecules helps relax the low vibrational levels, serves as a temporary storage of vibrational energy during the relaxation, and thereby delays the dissociation process, c) the dissociation and recombination rates can be approximated within an order of magnitude using equilibrium formulations and Park's two-temperature model for temperature averaging, d) lower vibrational levels tend to over-relax, and e) the average energy loss due to the dissociation is about 80–90% of the dissociation energy.

Nomenclature

D_0 = dissociation energy
$E(v)$ = energy of the vibrational level v measured with from the $v = 0$ level
e_v = average vibrational energy per molecule, cm^{-1}
$F(J)$ = rotational energy, cm^{-1}
h = Planck's constant
K_f = forward (dissociation) reaction rate coefficient, in $cm^3\ s^{-1}$
K_r = reverse (recombination) reaction rate coefficient, $cm^6\ s^{-1}$
$K(v; c)$ = transition rate coefficient for $v \rightarrow c$ (continuum) transition, $cm^3\ s^{-1}$
$K(v, J; c)$ = transition rate coefficient for $v, J \rightarrow c$ (continuum) transition, $cm^3\ s^{-1}$
$K(v, J; v', J')$ = transition rate coefficient for $v, J \rightarrow v', J'$ transition, in $cm^3\ s^{-1}$
$K(v; v')$ = transition rate coefficient for $v \rightarrow v'$ transition, $cm^3\ s^{-1}$
k = Boltzmann constant
$M(v)$ = second moment of vibrational transition rate, see Eq. (26)
m_μ = reduced mass of colliding molecules
N = number density
n = temperature exponent in rate coefficient
p = pressure in atmosphere
Q_{tA}, Q_{tB} = translational partition function for atoms A and B, respectively
Q_J = partition function for rotational level J
Q_v = partition function for vibrational level v
T = translational temperature
T_a = geometrical mean temperature
T_d = characteristic temperature of dissociation
T_v = vibrational temperature
$T_v(v)$ = definition of vibrational temperature in a nonequilibrium flow based on the populations of vibrational levels v and 0
t = time, seconds
V = interaction potential between two colliding molecules
v = vibrational quantum number
Δv = change in v
ε = average vibrational energy removed from the molecule per each dissociation event
θ = characteristic vibrational temperature = $\{E(1) - E(0)\}/k = 6320.0$ K
μ = reduced mass of colliding particles in atomic mass units
ρ_A, ρ_B = normalized population density of atoms A and B, respectively
ρ_v = normalized population density at vibrational level v
$\rho_{v,J}$ = normalized population density at rotational level J of the vibrational level v
τ_L = relaxation time deduced from the Landau-Teller equation

Subscripts

A = atoms A
B = atoms B
E = equilibrium
i = initial condition
J = rotational level J
v = vibrational level v
x = molecule

Presented as Paper 89-1738 at the AIAA 24th Thermophysics Conference, Buffalo, NY, June 12–14, 1989; received Aug. 31, 1989; revision received Aug. 15, 1990; accepted for publication Oct. 25, 1990.

*Research Scientist, Mail Stop 230-2. Associate Fellow AIAA.
†Research Scientist. Member AIAA.

Introduction

IN A recent publication,[1] we reported a theoretical study of vibrational excitation and dissociation of nitrogen molecules undergoing a nonequilibrium relaxation process upon heating and cooling. Using an extension of the theory originally proposed by Schwarz, Slawsky, and Herzfeld (SSH),[2]

bound-bound and bound-free transition probabilities were computed in that work. Based on these transition probabilities the master equation was numerically integrated to determine the population distributions of all the 57 vibrational states as well as the bulk thermodynamic properties. Rate coefficients for collisionally induced vibrational transitions and transitions from a bound state into a dissociative state were calculated. The most striking feature in those calculations was a deep minimum in the vibrational transition rates. This minimum was found to create a bottle neck in the transfer of vibrational energies between the lower vibrational states and the upper states, leading to a bi-modal distribution of the vibrational states. The vibrational distribution was severely distorted from the Boltzmann distribution in both heating and cooling cases. This was contrary to the Coupled-Vibration-Dissociation (CVD)[3] and Coupled-Vibration-Dissociation-Vibration (CVDV)[4] models previously put forward.

One main limitation of this work is in the neglect of rotational motion. Rotation can change vibrational transition rates in two different ways. First, it changes the shape of the vibration potential. In the high temperature range, the majority of the molecules are at a high-rotational quantum number. When the rotational motion is excited to this extent, the effective interactive potential is shifted upward, reducing the effective dissociation energy and producing a rotational barrier. The bound-bound and bound-free transition rates will be affected, at least, quantitatively, though their general behavior may remain the same. The second rotational effect involves rotational energy transfer. Here the rotational mode acts both as an energy reservoir and dump. It was our belief that the neglect of rotational energy transfer[1] would not cause significant changes in the resonant vibration-to-vibration (V-V) transitions but the effect on nonresonant (V-V) and vibration-to-translation (V-T) transitions will be stronger. Since the resonant V-V transitions dominate the overall transition rates and are the source of the observed bottleneck, we expected the neglect of rotational energy transfer would not affect the qualitative nature of the reported results.

In order to verify our assumptions, it became necessary to explore the effects of rotation on the coupled vibration-dissociation rates. In the present paper we will do that, i.e., extend our previous analysis to include finite rotational excitation of the molecules. Since N_2 has thousands of rotational states and the computations of the state-to-state transition rates were going to be a very difficult task, even with modern computation facilities, we concentrated our efforts, for the study of rotational effects on the coupled vibration-dissociation rate constant, on the H_2 molecule. The H_2 molecule is the simplest molecule to compute. Furthermore at NASA Ames Research Center, we already have computed the state-to-state transition rates for the H_2 molecule using a quasi-classical trajectory method.[5] Under these conditions, the H_2 molecule was a natural choice for this extension of our study of nonequilibrium hypersonic flows.

There is another very important motivation for the selection of H_2 as the molecule for this investigation. In recent years there has been a surge of interest in supersonic combustion ramjet (SCRAM-jet) engines for use in hypersonic civilian and military air transport systems. H_2 has been proposed as the fuel for the SCRAM-jet engines. Dissociation behavior of H_2 may affect the performance of such engines.

In the present paper we will explore the following points:

1) How are the vibrational and rotational states populated and what are the corresponding characteristic vibrational temperatures during the relaxation period?

2) What are the relaxation rates for the characteristic vibrational temperatures? Which model is the most accurate?

3) How are the dissociation and the recombination rates related to the characteristic vibrational temperatures? Which model is the most accurate?

4) What is the value of the average vibrational energy removed during dissociation? and

5) How does the inclusion of the rotational degree of freedom in the computation change the parameters mentioned above?

To focus the study on the effect of the resonant V-V energy transfers, we assume that the colliding particle is always a molecule.

The relaxation phenomena have been studied theoretically for two typical cases. The first is a heating case wherein the gas, initially in equilibrium at T_0, is heated suddenly to TK. In the second case, the gas is cooled from the initial temperature of T_0 to TK. A constant-volume, isothermal condition was assumed during the relaxation process. The rate equations for the change of the rotational state and the vibrational state populations, that is, the master equations, are integrated in time for these two cases with the use of the computed transition rate coefficients. In addition to the rotational model, a rotationless[1] model is also constructed and the computations are repeated using this rotationless model.

The state-to-state transition rates are computed by a quasi-classical trajectory method. The calculation yields a complete set of transition rate coefficients among all combinations of initial and the final rotational and vibrational, and/or free states. The integration of the master equations yield the population distribution of all rotational and vibrational states as a function of time as well as the number densities of the atoms and molecules. From these rotational and vibrational distributions, the vibrational temperature, the forward (dissociation) and reverse (recombination) rate coefficients, the average vibrational energy e_v, average rotational energy e_R, the average combined vibrational-rotational energy e_{vR}, and the average transferred energy ε are calculated. The dissociation rate coefficients are also calculated using Park's model, and comparison is made between these values and the results from the time integration. For illustration purposes the vibrational population from both the rotational as well as rotationless model are expressed as vibrational temperatures computed with respect to the ground state population, and are compared with the Landau-Teller prediction. The Landau-Teller model,[6] expressed in terms of the average vibrational energy per molecule, $e_v(T_v)$, is given by

$$\frac{\partial e_v(T_v)}{\partial t} = \frac{e_{vE}(T) - e_v(T_v)}{\tau_L} \tag{1}$$

where τ_L in seconds is given by[7]

$$\tau_L = 1/p \exp[A(T^{-1/3} - 0.015\mu^{1/4}) - 18.42]$$

T is the translational temperature, μ is the reduced mass of the two colliding particles in atomic mass units, and p is the pressure in atmosphere. The quantity A is given by

$$A = 1.16 \times 10^{-3}\mu^{1/2}\theta^{4/3}$$

and θ is the characteristic vibrational temperature

$$\theta = [E(1) - E(0)]/k$$

Here $E(0)$ and $E(1)$ are the energies of the ground and first excited vibrational levels (relative to the minimum in the vibrational potential), and k is the Boltzmann constant.

The transition rate coefficients calculated in the present work show that the transitions are very fast among the high vibrational states and between the high vibrational states and the free state. This drives the population distribution into a distinct dual-mode in which the lower and the higher states reach separate quasi-equilibrium distributions. Although there is no apparent minimum in the transition rates as was seen in Ref. 1, a decoupling of the relaxation of the upper states and lower states is seen. Park's two-temperature model[8] is

seen to agree with the detailed calculation to within an order of magnitude with

$$T_a = T_v^{0.5} T^{0.5} \tag{2}$$

The average vibrational energy transferred in dissociation ε is found to be 80–90% of D_0, much larger than predicted by the CVDV[4] and the preferential removal theories[9] and in contrast to previous finding for N_2.

Computation of Transition Rate Coefficients

The state-to-state rate coefficients for this study have been determined using the quasi-classical trajectory method. This requires as input a potential energy function which describes the interaction of the two hydrogen molecules. For the present work, the potential of Ref. 5 is used. This potential is a multiparameter analytic representation of the results of extensive ab initio electronic structure calculations, and is expected to faithfully reflect the properties of the accurate potential.

All quantum states of H_2 are assigned using the WKB method[10]; this yields 348 bound and quasibound v, J levels (Table 1). For each of the 348 levels, 2000 trajectories were integrated using the variable step-size algorithm of Ref. 5. Approximately one tenth of the trajectories were back integrated to monitor the suitability of the numerical parameters controlling the accuracy of the solutions. Most of the trajectories were evaluated using the NAS facility Y-MP, and 2000 trajectories required from 15 min (T = 10,000 K) to 45 min (T = 1000 K) of CPU time.

The initial conditions for the trajectories were selected as in Ref. 5 with the exception that one maximum impact parameter was used (12, 10, 10, and $8a_0$ [$1a_0 = 5.291771 \times 10^{-9}$ cm] for 1000 K, 2000 K, 5000 K, and 10,000 K, respectively), and the initial states were fixed. The initial state for the target was one of the 348 levels, and the initial state for the projectile was taken as the most likely state from a thermal distribution consisting only of molecules having J even (odd) if the target J was odd (even).

The final states of the target were assigned using the histogram method[10] while the final states of the projectile were summed over. This yields rates for all processes of the form

$$H_2(v, J) + M \rightarrow H_2(v', J') + M \tag{3}$$

and

$$H_2(v, J) + M \rightarrow H + H + M \tag{4}$$

This determines all state-to-state rate coefficients except the ones for free-to-bound transitions. These are generated from the bound-to-free transition rate coefficients by using microscopic reversibility. Finally, to ensure that the proper equilibrium is reached, all bound-bound state-to-state rate coefficients for endoergic transitions are replaced with the values calculated using microscopic reversibility from the reverse transitions.

Table 1 Characterization of the vibrational levels of H_2

v	$E^*(v)$, cm^{-1}	J_{max}
0	0.0	39
1	4162.0	36
2	8088.5	34
3	11784.4	32
4	15252.9	30
5	18495.0	28
6	21509.3	26
7	24291.9	24
8	26835.3	22
9	29128.4	19
10	31154.5	17
11	32890.6	15
12	34304.5	12
13	35351.5	9
14	35969.8	5

*Energies are with respect to the v = 0 state, which is at 2344.6 cm^{-1} above the minimum of the potential curve.

Formulations of Rate Equations

Temporal Variation in Vibrational State Populations

We will designate the H_2 molecule with the suffix x and the two atoms resulting from its dissociation by the suffices A and B, even though they are identical. We consider that the mixture containing the species x, A, and B is confined in a box of unit volume. At times prior to t = 0, equilibrium existed at a specified temperature T_0. At time t = 0, the gas is suddenly heated or cooled by an unspecified means so that the translational temperature acquires a new value T. The box is, henceforth, maintained at an isothermal condition. Due to the suddenly changed T, collisional processes occur to vibrationally excite or de-excite to relax to a condition appropriate to T. Some of the collisions lead to a free-bound (dissociation or recombination) transition $v, J \rightleftharpoons A + B$. The state $A + B$ will be designated by c (continuum). There are a total of 15 vibrational states starting from v = 0 to v = 14, and a total of 348 rotational states with 39 rotational states at v = 0 and 5 rotational states at v = 14. It is further assumed that the ionization level is small and the bound-bound collisional transitions occur only when both colliding partners are molecules. In this manner, we can focus our study to the effect of the resonance transitions in V-V energy transfer, a dominant process in the typical flow regime around a hypersonic vehicle.

The number density of those molecules in the rotational state J of the vibrational state v, or population, $N_{v,J}$, is affected by the incoming and outgoing rates. An incoming rate is the rate of an individual transition from an initial rotational state J' of the vibrational state v' or a free state c via collisions with the colliding particle x. When the initial state is a bound rotational state, the rate is given by $K(v', J'; v, J)N_{v',J'}N_x$, where $K(v', J'; v, J)$ is the rate coefficient for the transition $(v', J') \rightarrow (v, J)$ given in the units of cm^{3}s^{-1}. When the initial state is the free state, its rate is given by $K(c; v, J)N_AN_BN_x$. An outgoing rate is its reverse, $K(v, J; v', J')N_{v,J}N_x$ or $K(v, J; c)N_{v,J}N_x$. The time rate of change of $N_{v,J}$ is the difference between the sum of all incoming rates and the sum of all outgoing rates

$$\frac{\partial N_{v,J}}{\partial t} = N_x \sum_{v'} \sum_{J'} K(v', J'; v, J)N_{v',J'} + K(c; v, J)N_AN_BN_x - N_x \sum_{v'} \sum_{J'} K(v, J; v', J')N_{v,J} - K(v, J; c)N_{v,J}N_x. \tag{5}$$

We introduce $N_{(v,J)E}$, the equilibrium population of the state v, J for a given total molecule density N_x

$$N_{(v,J)E} = N_{xE}\frac{Q_vQ_J}{Q_x}, \qquad N_v = \sum_J N_{v,J} \tag{6}$$

$Q_x = \Sigma_v Q_v(\Sigma_J Q_J)$ is the vibrational-rotational partition function of the molecule, Q_v is the vibrational partition function of the state v and Q_J the rotational partition function of the state J

$$Q_v = \exp\{-E(v)/kT\}$$
$$Q_J = g_J(2J + 1)\exp\{-F(J)/kT\} \tag{7}$$

k is the Boltzmann constant, and

$$g_J = \begin{cases} 1, & J \text{ even} \\ 3, & J \text{ odd} \end{cases} \tag{8}$$

$E(v)$ and $F(J)$ are the vibrational and rotational energies measured with respect to the ground state, respectively. We further define the normalized populations ρ_v and $\rho_{v,J}$ by

$$\rho_{v,J} = \frac{N_{v,J}}{N_{(v,J)E}}, \qquad \rho_v = \frac{N_v}{N_{vE}} \tag{9}$$

For the free state, we define the normalized density ρ_A and ρ_B by

$$\rho_A = \frac{N_A}{N_{AE}}, \qquad \rho_B = \frac{N_B}{N_{BE}} \tag{10}$$

The equilibrium number densities, N_{AE} and N_{BE} are given by

$$\frac{N_{AE}N_{BE}}{N_x} = \frac{Q_{At}Q_{Bt}}{Q_{xt}Q_x} \exp\left(-\frac{D_0}{kT}\right)$$

Here, Q denotes a partition function as before, and the subscript t refers to the translational mode. We invoke the principle of detailed balancing between a forward and its backward rates under equilibrium, which leads to

$$K(v, J; v', J')N_{(v,J)E} = K(v', J'; v, J)N_{(v',J')E} \tag{11}$$

for the bound-bound transitions, and

$$K(v, J; c)N_{(v,J)E} = K(c; v, J)N_{AE}N_{BE} \tag{12}$$

for the bound-free transitions. By dividing Eq. (5) by $N_{(v,J)E}$, and using Eqs. (9) to (12), the master equation becomes

$$\frac{1}{N_x}\frac{\partial \rho_{v,J}}{\partial t} = \sum_v \sum_J K(v, J; v', J')(\rho_{v',J'} - \rho_{v,J}) + K(v, J; c)(\rho_A\rho_B - \rho_{v,J}) \tag{13}$$

The rate of change of the density of the atoms A and B and of the molecular density can be expressed as

$$\frac{\partial N_A}{\partial t} = \frac{\partial N_B}{\partial t} = -\frac{\partial N_x}{\partial t} = \sum_v \sum_J K(v, J; c)N_xN_{v,J} - \sum_v \sum_J K(c; v, J)N_AN_BN_x$$

Using the detailed balancing relationship Eqs. (11) and (12), and after some manipulation, we can rewrite the equation in the form

$$\frac{\partial(\rho_A\rho_B)}{\partial t} = 2\sqrt{\frac{\rho_A\rho_B}{(N_AN_B)_E}} \sum_v \sum_J K(v, J; c)N_xN_{(v,J)E} \times (\rho_{v,J} - \rho_A\rho_B) \tag{14}$$

The 348 equations from Eq. (13) and Eq. (14) must be integrated numerically to obtain $\rho_{v,J}$ and $\rho_A\rho_B$ as function of time. Solving 349 stiff equations simultaneously can be very time consuming, therefore, only 94 of these are selected and simultaneously solved. A stiff equation solver based on Bowen's work[11] is used for this purpose. After a few time steps the population densities for all the 348 bound and the free states are updated by interpolation. A typical solution requires about 5.5 h on Cray X-MP computer.

Characteristic Vibrational Temperatures

In a nonequilibrium flow, there is no unique vibrational temperature. However, one can define a vibrational temperature arbitrarily for a specific purpose. For illustration purposes the population density of the vibration level v may be expressed as vibrational temperatures $T_v(v)$

$$\frac{N(v)}{N(0)} \equiv \frac{N_E(v)}{N_E(0)}\frac{\rho(v)}{\rho(0)} = \exp\left[-\frac{E(v) - E(0)}{T_v(v)}\right]$$

Another vibrational temperature can also be defined which characterizes the average energy contained in the vibrational mode. Using the conventional harmonic oscillator expression, T_{ve} is defined from the average vibrational energy e_v as

$$e_v = \frac{k\theta}{\exp(\theta/T_{ve}) - 1} \tag{15}$$

where θ is the characteristic vibrational temperature. $\theta = \{E(1) - E(0)\}/k = 6320$ K. The energy e_v is determined in turn from the computed ρ_v by

$$e_v = \frac{\Sigma_v\Sigma_J E(v)n_{(v,J)E}\rho_{v,J}}{\Sigma_v\Sigma_J N_{(v,J)E}\rho_{v,J}}$$

This temperature is useful in displaying the amount of energy contained in the vibrational mode. The average rotational energy and the average combined vibrational-rotational energies are defined in the same manner.

Reaction Rate Coefficients

For relaxing gases it is customary to express the rate of change of number density in terms of bulk-rate coefficients K_f for the forward (dissociation) and K_r for the reverse (recombination) processes

$$\frac{\partial N_{A,B}}{\partial t} = K_fN_xN_x - K_rN_xN_AN_B \tag{16}$$

When the gas is in a highly nonequilibrium condition, one of the two terms of Eq. (16) is dominant over the other. In such a case, K_f or K_r can be determined approximately from

$$K_f \approx \frac{\partial N_{A,B}}{\partial t}\frac{1}{(N_x^2)} \tag{17}$$

or

$$K_r \approx \frac{\partial N_{A,B}}{\partial t}\frac{1}{(N_AN_BN_x)} \tag{18}$$

In general, K_f is a function of time because $\rho_{v,J}$ varies with time. If the $\rho_{v,J}$ distribution is uniquely determined by T and T_{v1}, then K_f can be expressed as functions of T and T_{v1} only. Such condition can exist if the high vibrational states are populated according to the quasi-steady-state (QSS) condition, that is, the left-hand-side of Eq. (13) is negligibly smaller in comparison with either of the two rates affecting $\rho_{v,J}$, namely, the sum of all incoming rates or the sum of all outgoing rates. Suppose that the QSS condition exists for the states above $v = v_s$ and $J = J_s$. Then, for these states, the master equation can be written as

$$\sum_{v_s}^{v_{max}} \sum_{J_s}^{J_{max}} K(v, J; v', J')\rho_{v',J'} - \sum_0^{v_{max}} \sum_0^{J_{max}} K(v, J; v', J')\rho_{v,J} - K(v, J; c)\rho_{v,J} = -K(v, J; c)\rho_A\rho_B - \sum_0^{v_s} \sum_0^{J_s} K(v, J; v', J')\rho_{v',J'} \tag{19}$$

If the states below v_s, J_s are populated according to the Boltzmann distribution at a vibrational and a rotational temperature T_{v1} and T_{r1}, then the second term on the right-hand side becomes a function only of T, T_{r1} and T_{v1}. In that case, the solution to the algebraic Eq. (19) can be written as

$$\rho_{v,J} = \rho^h_{v,J}(T) + \rho_A\rho_B\rho^p_{v,J}(T, T_{v1}, T_{r1}) \tag{20}$$

where ρ^h is the homogeneous solution of Eq. (19) and ρ^p a particular solution.

Using the detailed balance relationship of Eqs. (11) and (12) the overall reaction rate can now be written and compared with Eq. (16), one finds

$$K_f = \sum_{v_s}^{v_{max}} \sum_{J_s}^{J_{max}} K(v, J; c) \frac{Q_v Q_J}{Q_x} \rho^h_{v,J} \tag{21}$$

$$K_r = \sum_{v_s}^{v_{max}} \sum_{J_s}^{J_{max}} K(v, J; c) \frac{N_x}{N_{AE}N_{BE}} \frac{Q_v Q_J}{Q_x} (1 - \rho^p_{v,J}) \tag{22}$$

Equations (21) and (22) are valid even when the flow is close to or at equilibrium. These equations are used in the present work whenever appropriate.

Average Vibrational Energy Loss Due to Dissociation

When a gas molecule with the vibrational energy $E(v)$ dissociates by collision with another particle, the vibrational energy content of the gas is reduced by an amount equal to $E(v)$. As pointed out by Marrone and Treanor,[9] dissociation occurs preferentially from the upper vibrational states. Thus, even a single dissociation depletes the vibrational energy by an amount nearly equal to the dissociation energy of the molecule. The rate of energy loss by a transition from the rotational level J of the vibrational level v is $K(v, J; c)E(v)N_{v,J}N_x$. Conversely, the reverse process of recombination into the rotational level J of the vibrational level v adds a vibrational energy equaling $K(c; v, J)E(v)N_AN_BN_x$. The average vibrational energy loss ε can be defined by

$$\begin{aligned} -\varepsilon \frac{\partial N_x}{\partial t} &= \sum_v \sum_J E(v)K(v, J; c)N_{v,J}N_x \\ &\quad - \sum_v \sum_J E(v)K(c; v, J)N_AN_BN_x \\ &= N_xN_{xE} \sum_v \sum_J E(v)K(v, J; c) \frac{Q_vQ_J}{Q_x} (\rho_{v,J} - \rho_A\rho_B) \end{aligned} \tag{23}$$

In terms of ρ_v, the average vibrational energy loss rate is

$$\varepsilon = \frac{\Sigma_v\Sigma_J E(v)K(v, J; c) \frac{Q_vQ_J}{Q_x} (\rho_{v,J} - \rho_A\rho_B)}{\Sigma_v\Sigma_J K(v, J; c) \frac{Q_vQ_J}{Q_x} (\rho_{v,J} - \rho_A\rho_B)} \tag{24}$$

Diffusion Approximation

In the high temperature regime where the kinetic energy kT is larger than the vibrational energy gap, collisional excitation and de-excitation of the vibrational states occur almost in accordance with the classical mechanics. According to the classical concept, the vibrational levels are considered to be continuously distributed. Keck and Carrier[12] have shown that under these assumptions this equation can be converted into a diffusion equation of the form

$$\frac{1}{N_x}\frac{\partial \rho(v)}{\partial t} = \frac{\partial}{\partial v}\left(M(v)\frac{\partial \rho(v)}{\partial v}\right) + K(v; c)\{\rho_A\rho_B - \rho(v)\} \tag{25}$$

where M, the second moment of vibrational transition, is defined as

$$M(v) = \frac{1}{2}\int_{-\infty}^{+\infty} K(v; v + \Delta v)(\Delta v)^2 d(\Delta v) \tag{26}$$

A complete derivation of the diffusion formulation is given in Ref. 1. In the present calculation the diffusion equation is not solved but the second moment of the vibrational transitions $M(v)$ is used for comparative and illustrative purposes.

Results

Behavior of Transition Rate Coefficients

The calculated values of the bound-bound transition rate coefficient $K(v, J; v', J')$ cannot be shown in a single figure because there are $348 \times 348 = 121{,}104$ such values. However, there are only 15 values each for the second-moment of transition rate coefficient, $M(v)$, and the bound-free transition rate coefficient, $K(v; c)$. $M(v)$ values are computed using Eq. (26), and $K(v; v')$ are obtained by summing up the rates over the rotational states for each vibrational state. The rotational states are assumed to be populated according to the Boltzmann distribution at the equilibrium temperature. $K(v; c)$ rates are also obtained in a similar manner. $M(v)$ and $K(v; c)$ are shown in Fig. 1 for the case where $T = 3000$ K. The rotational states of the colliding particles are assumed to be in a Boltzmann distribution at this temperature. Since $M(v)$ is a sum of the rates from all the states, it is a better indicator of the overall rate of transition. The $M(v)$ values for the Landau-Teller model are also shown in the figure for comparison.

As seen from the plot, the transition moment $M(v)$ based on the Landau-Teller model increases monotonically with the vibrational levels. This is due to the fact that $K(v; v + 1)$ is proportional to $v + 1$ in the Landau-Teller model. The transition moments $M(v)$ based on the trajectory calculations increase with the vibrational level at a much faster rate than the Landau-Teller values. This monotonical increase in $M(v)$ over Landau-Teller values can be primarily attributed to the rotational effects. At high temperatures even the lower vibrational levels are populated by molecules with high rotational quanta. Thus, the average transition rate from a given

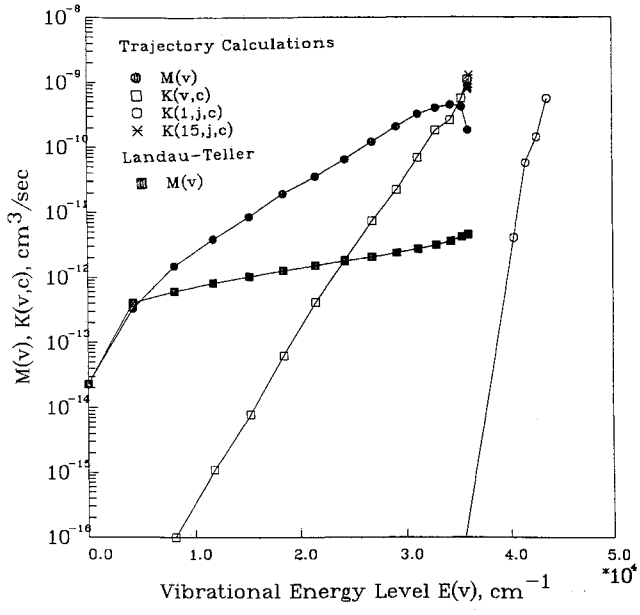

Fig. 1 The second moment of vibrational transition rate coefficients $M(v)$ and the bound-free transition rate coefficient $K(v; c)$, compared with $M(v)$ for the Landau-Teller model; $T = 3000$ K. The colliding particles are assumed to be in the rotational states most probable for $T = 3000$ K.

vibrational level tends to be higher than that of a rotationless molecule. Most notable point here is that there is no apparent bottleneck (minimum) in the $M(v)$ function as was found in the rotationless model[1] for N_2. This bottleneck in the case of nitrogen caused higher vibrational levels to equilibrate among themselves and with the free state and the lower levels with the ground state, but with a weak coupling between the two groups. In the present case with a monotonically increasing $M(v)$, one would expect the coupling between the vibrational states becoming stronger and stronger as we move towards the free state, being strongest near the free state. In other words from midlevels down to the ground state the interstate coupling grows weaker and weaker. The peak bound-free transition rate coefficient $K(v; c)$ is $\sim 10^{-9}$ cm^3/s for $v = 14$ ($E(v) = 35{,}970$ cm^{-1}). These rates decrease very rapidly with decreasing vibration quanta, suggesting that overall forward reaction rate is going to be slower. However, as seen by the tail-end of the plots of $K(0, J; c)$ and $K(14, J; c)$, the contribution to dissociation is going to be from all vibrational levels.

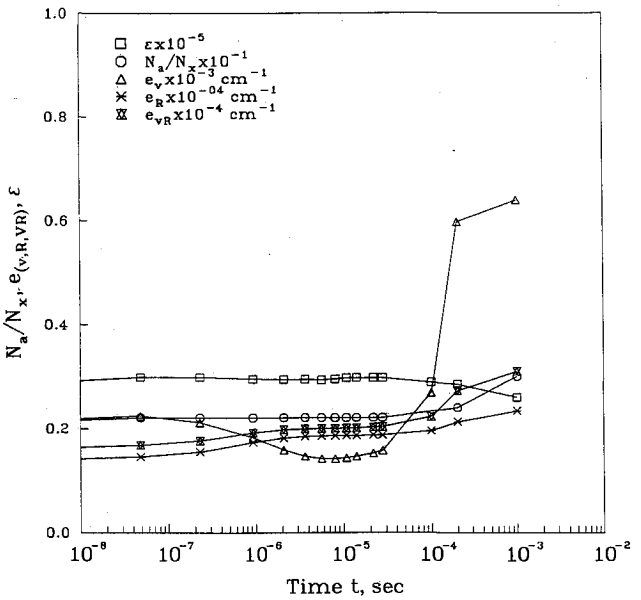

Fig. 2a Temporal variations of the bulk thermodynamic properties in a heating environment ($T_0 = 2000$ K $\rightarrow T = 3000$ K): the ratio of atoms to molecule densities N_A/N_x, average vibrational energy per molecule e_v, average rotational energy per molecule e_R, average vibrational-rotational energy per molecule e_{vR}, and average vibrational-rotational energy removed in a dissociation (rotational model).

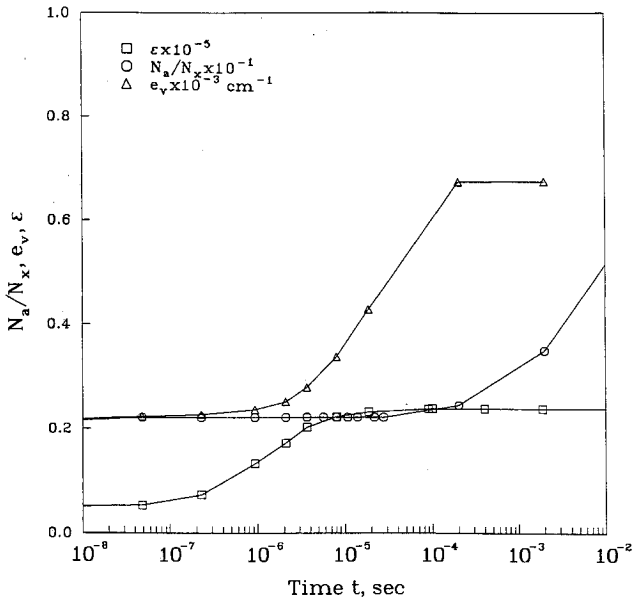

Fig. 2b Temporal variations of the bulk thermodynamic properties in a heating environment ($T_0 = 2000$ K $\rightarrow T = 3000$ K): the ratio of atoms to molecule densities N_A/N_x, average vibrational energy per molecule e_v, average rotational energy per molecule e_R, average vibrational-rotational energy per molecule e_{vR}, and average vibrational-rotational energy removed in a dissociation ε (rotationless model).

Relaxation Behavior in Heating Environment

The normalized population densities $\rho_{v,J}$ for all the 348 rotational states and ρ_v for all the vibrational states were computed for heating and cooling environments by integrating the master equation, Eq. (13) and the accompanying equation for $\rho_A\rho_B$, Eq. (14), in time. For illustrative purposes, solutions for a rotationless model were also obtained by solving another set of equations, similar to Eqs. (13) and (14) (see Ref. 1). For the heating case, it was assumed that the gas mixture was in equilibrium at $T = 2000$ K, then at $t = 0.0$ s, the gas mixture is heated to $T = 3000$ K. Vibrational excitations and dissociations are allowed to occur at a constant volume, isothermal condition thereafter. The initial number densities for the molecules and atoms were 10^{17} and 10^6 cm^{-3}, respectively. The calculated values of the normalized number density, N_A/N_x, the average dissociation energy loss, ε, the average vibrational energy, e_v, the average rotational energy, e_R, and average vibrational-rotational energy, e_{vR}, are plotted Fig. 2a as functions of time. As seen from the figure, the average energy loss due to dissociation starts from 29,918 cm^{-1} at $t = 0.0$ s and levels off to a value of 28,567 cm^{-1}. The final value being about 79% of the dissociation energy. Although these values are considerably larger than the $D_0/2$ predicted by CVDV[4] theory and certainly smaller than the preferential removal theory,[9] this result is not surprising. Blais and Truhlar[13] have reported similarily high energy of activation for collisions leading to complete dissociation, while studying the effects of rotational energy on dissociation. In other words, it appears that such a high energy loss due to dissociation is primarily due to rotational effects. The average vibrational energy initially decreases with time, then rises quickly around $t = 10^{-4}$ s to a value approaching 650 cm^{-1}. The average rotational and the combined rotational-vibrational energies increase with time, and after $t = 10^{-4}$ s both achieve constant values, i.e., $e_R = 2320$ cm^{-1} and $e_{vR} = 2970$ cm^{-1}. At this time the atomic number density starts to slowly rise. The bulk properties computed by the rotationless model are shown in Fig. 2b. In this case one finds that the average vibrational energy removed in dissociation increases with time to achieve a constant value of 23,794 cm^{-1}, about 66% of the dissociation energy at $t > 10^{-4}$. The average vibrational energy increases to a final value of 675 cm^{-1}, almost equal to e_v for the rotational model.

The normalized vibrational population densities as a function of the vibrational levels at selected times from the rotational model are shown in Fig. 3a. As the time passes, the populations at mid-levels, moving towards the equilibrium value, becomes independent of v. This behavior indicates that the mid-vibrational levels equilibrate among themselves. The higher levels lag slightly behind and are not in equilibrium with each other. The lower vibrational levels, however, over relax, falling below the equilibrium value. To examine this peculiar behavior of the lower levels, the rotational populations for $v = 0$ and 14 are plotted in Fig. 3b. As seen from the Fig. 3b the rotational levels below $J = 8$ quickly relax towards their equilibrium value. The rotational levels in the range $J = 12$–31 also tend to approach the equilibrium but at different speed. The levels above $J = 31$ show a strong nonequilibrium effect with $J = 38$ moving very slowly towards the equilibrium. The rotational levels of $v = 14$ relax at a fast rate. The normalized populations from the rotationless model are plotted in Fig. 3c. In this model the lower levels

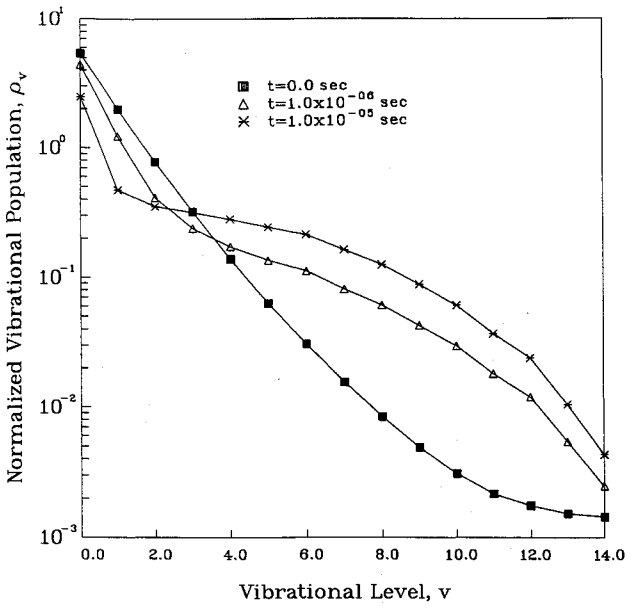

Fig. 3a Normalized vibrational population density as a function of the vibrational level, v, at selected times, in a heating environment, T_0 = 2000 K → T = 3000 K (rotational model).

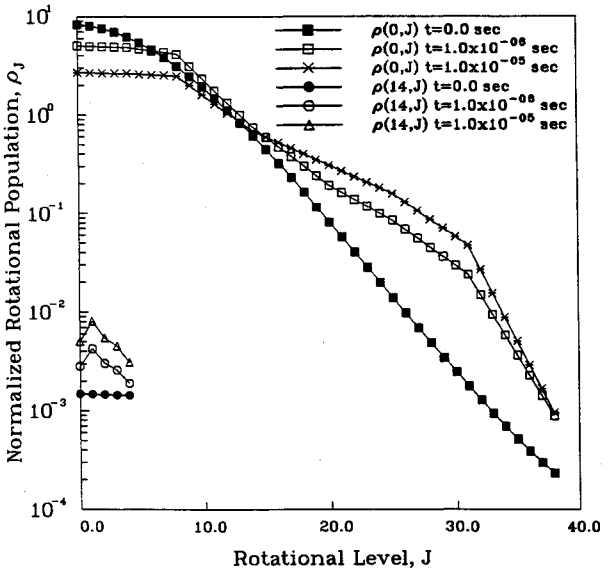

Fig. 3b Normalized rotational population $\rho_{v,J}$ for v = 0 and 14 as a function of the vibrational levels, v, at selected times, in a heating environment, T_0 = 2000 K → T = 3000 K (rotational model).

relax relatively quickly towards the equilibrium value with the higher vibrational levels slightly lagging behind.

For illustrative purposes, the vibrational population is expressed as the vibrational temperature, with respect to the population at v = 0. These vibrational temperatures as a function of time for the rotational and rotationless models are shown in Figs. 4a and 4b, respectively. In these figures the vibrational temperatures $T_v(1)$, $T_v(8)$, and $T_v(14)$ are compared with the Landau-Teller prediction. As seen from Fig. 4a, the Landau-Teller theory predicts that the relaxation is almost over at $t = 6 \times 10^{-5}$ s. However, all four temperatures from the calculated solution converge only after $t = 2 \times 10^{-4}$ s near the equilibrium temperature. Interestingly, the vibrational temperature based on the average vibrational energy and based on v = 1 fall below the initial temperature, then quickly catch up with other vibrational temperatures after $t > 4 \times 10^{-5}$ s. In other words, the midlevels approach the equilibrium temperature at a steady pace with the higher vibrational levels slightly lagging behind. However, the vibrational temperature based on the lower levels as well as on the average vibrational energy, become, initially, depressed below the initial value, then quickly rise to approach their equilibrium values. In the rotationless model (Fig. 4b), all the temperatures except that based on v = 14 follow the Landau-Teller prediction.

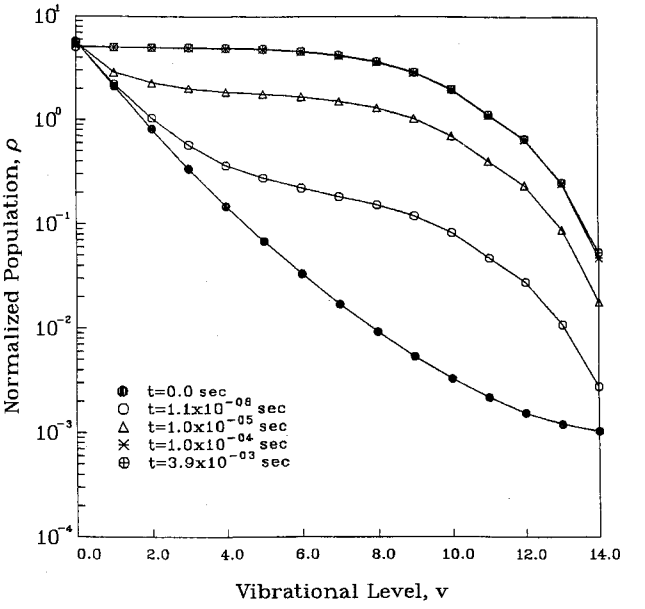

Fig. 3c Normalized vibrational population ρ_v as a function of the vibrational level, v, at selected times, in a heating environment, T_0 = 2000 K → T = 3000 K (rotationless model).

Finally the computed dissociation rates K_f as a function of time are plotted in Fig. 5a. For comparison best estimates from the empirical relationship given by Cohen and Westberg[13]

$$K_f = 1.43 \times 10^{-6}\, T^{-0.7} \exp(-52530/T_a) \qquad (27)$$

are also plotted in this figure. The temperature T_a is calculated by using the Park model $T_a = \sqrt{(TT_v)}$. Three T_vs are selected, based on v = 1, 8, and 14 in relation to the population at v = 0. The calculated dissociation rates computed up to $t \sim 10^{-6}$ are for a highly nonequilibrium regime. It is not possible to compare them with the data based on experimental measurements, since the measurements can not resolve the times shorter than 10^{-6} s. For $t > 10^{-6}$, the estimates from the empirical data are within one order of magnitude in relation to the exact rates, except the one based on v = 1. If one puts a smaller weight on the equilibrium temperature T in the Park model, such as $T_a = T^{.7}T_v^{.3}$, better agreement between the exact solution and the experimental data may be found. Similar comparison for the dissociation rates, based on the rotationless model, are made in Fig. 5b. The dissociation rates predicted by the rotationless model seems to differ by several orders of magnitude, except near equilibrium.

There are two major observations that can be made by comparing the rotational and rotationless models: 1) overall dissociation rates predicted by the rotationless model are at least one order of magnitude higher than predicted by the rotational model and 2) overall agreement between the calculated rates and those based on empirical[13] relationship is much better in the rotational model.

Relaxation Behavior in Cooling Environment

In the cooling case, the gas is assumed to be in equilibrium in the beginning at T = 2000 K with the molecular and atomic number densities of 10^{17} and 2.25×10^{15} cm^{-3}, respectively. At t = 0 s, the gas mixture is cooled to 1000 K by an unspecified method, and is held at a constant volume, isothermal conditions thereafter. The process is very similar to that occurring in an expanding nozzle. The bulk thermodynamic

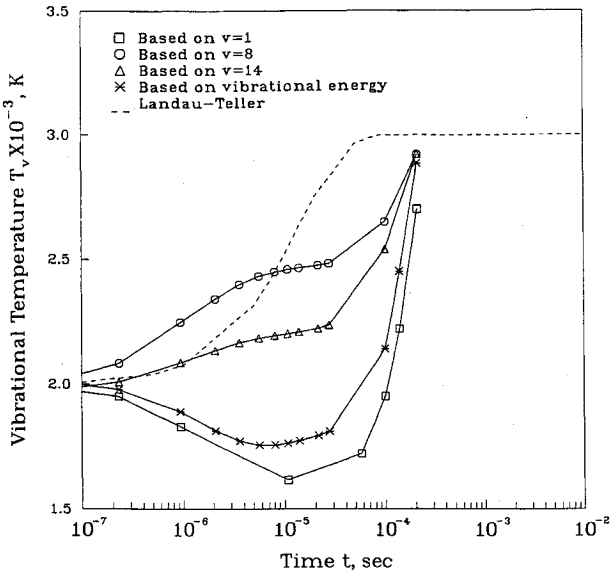

Fig. 4a Variation of the vibrational temperature based on v = 2, 8, and 14, and vibrational energy content, compared with the Landau-Teller prediction, in a heating environment, T_0 = 2000 K → T = 3000 K (rotational model).

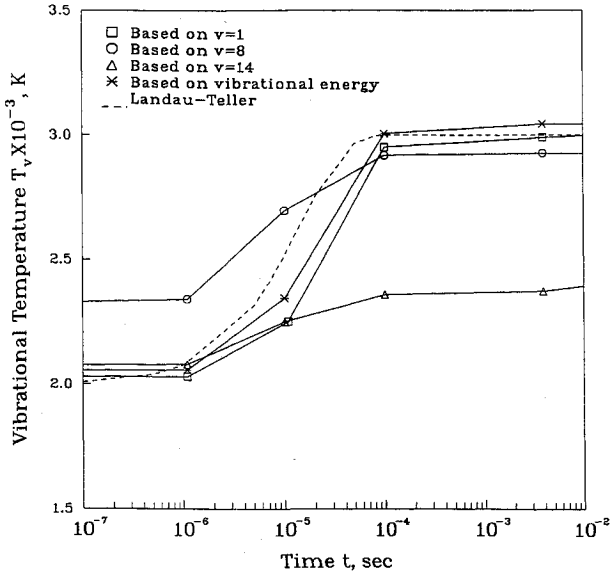

Fig. 4b Variation of the vibrational temperature based on v = 2, 8, and 14, and vibrational energy content, compared with the Landau-Teller prediction, in a heating environment, T_0 = 2000 K → T = 3000 K (rotationless model).

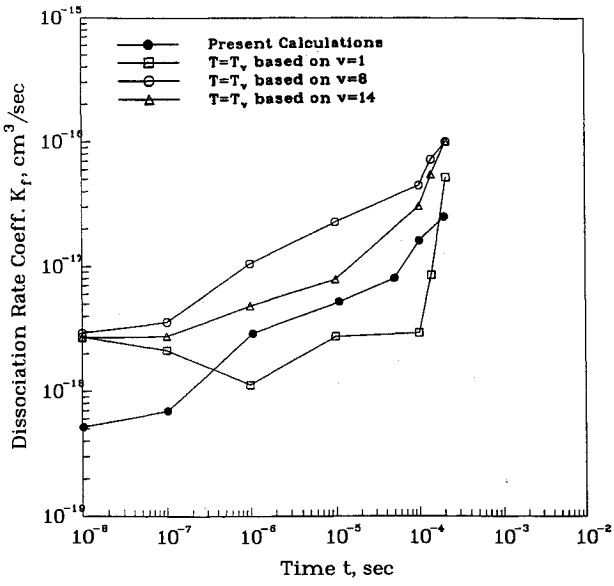

Fig. 5a The calculated dissociation rate coefficient K_f compared with Park model, in a heating environment T_0 = 2000 K → T = 3000 K (rotational model).

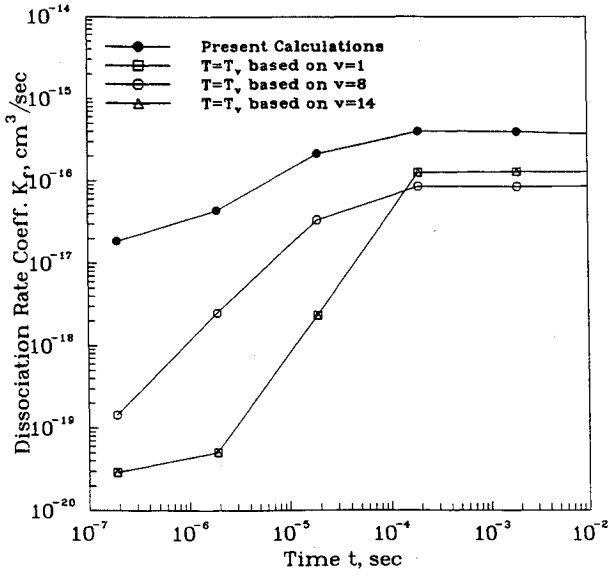

Fig. 5b The calculated dissociation rate coefficient K_f compared with Park model, in a heating environment T_0 = 2000 K → T = 3000 K (rotationless model).

properties, N_A/N_x, ε, e_v, e_R, and e_{vR} are plotted as functions of time in Fig. 6a. The average vibrational energy gain due to recombination starts from a value of 33,894 cm^{-1} at t = 0 s, slowly decreases with relaxation, and achieves a value of 32,470 cm^{-1} at $t = 2.4 \times 10^{-4}$ s, about 90% of the dissociation energy. The average vibrational energy starts from a low value of 236.5 cm^{-1} at t = 0.0 s and rapidly increases to high value of 1208.7 cm^{-1} at $t = 2.4 \times 10^{-4}$ s which is about 5.4 times higher than that predicted by the rotationless model shown in Fig. 6b. The average rotational energy in the rotational model starts from 1413.0 cm^{-1} and decreases to 702.9 cm^{-1} at $t = 2.4 \times 10^{-4}$ s. The combined average energy increases from 1658.8 to 1911.5 cm^{-1}. The average gain due to recombination in the rotationless model, as seen in Fig. 6b, is about 30351.0 cm^{-1} or 85% of the dissociation energy.

The normalized vibrational population as a function of the vibrational level at selected times as computed by the rotational model is shown in Fig. 7a. The higher vibrational levels initially exhibit some degree of population inversion and then revert back to their original approach towards the equilibrium. The lower states remain in a population inversion mode for a long time. This situation can be observed more clearly in Fig. 7b where the rotational population for the vibrational level v = 0 and v = 14 are plotted.

As seen from Fig. 7b, at v = 0, the lower rotational levels are inverted but the upper rotational levels are relaxing. For v = 14, all the rotational levels are inverted. This suggests that the rotation tends to relax the molecules.

Figure 7c depicts the ρ_v from the rotationless model. The relaxation does seem to occur very slowly in the lower vibrational levels. The higher levels, on the other hand, depict a strong population inversion.

In Figs. 8a and b the vibrational temperatures $T_v(v)$ as functions of v are shown for the rotational model and rotationless model, respectively. In the rotational model a uniform relaxation of the higher levels is clearly seen, which was less obvious in Fig. 7a. The lower vibrational levels are highly inverted. However, in the rotationless model the population

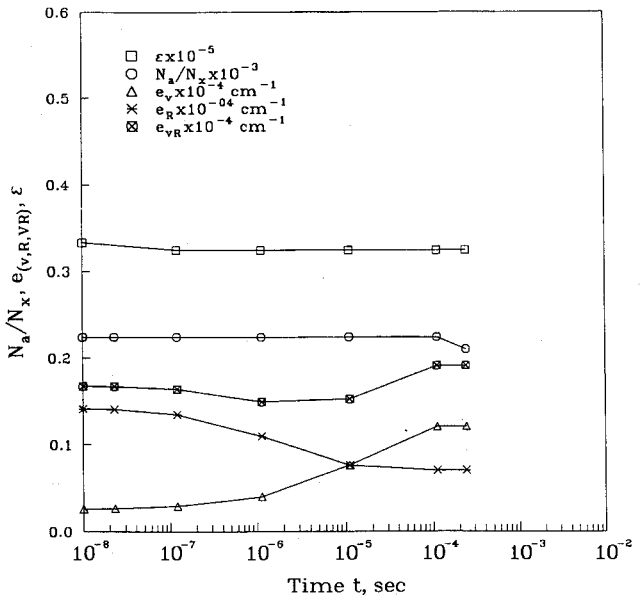

Fig. 6a Temporal variations of the bulk thermodynamic properties in a cooling environment (T_0 = 2000 K → T = 1000 K): the ratio of atoms to molecule densities N_A/N_x, average vibrational energy per molecule e_v, average rotational energy per molecule e_R, average vibrational-rotational energy per molecule e_{vR}, and average vibrational-rotational energy removed in a dissociation ε (rotational model).

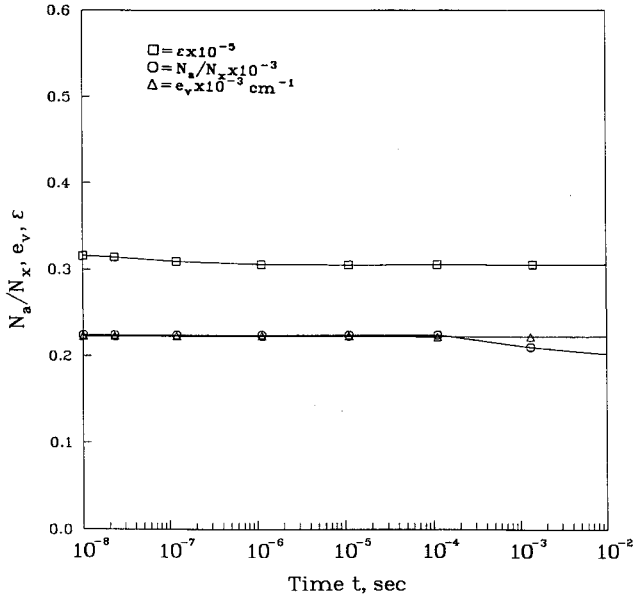

Fig. 6b Temporal variations of the bulk thermodynamic properties in a cooling environment (T_0 = 2000 K → T = 1000 K): the ratio of atoms to molecule densities N_A/N_x, average vibrational energy per molecule e_v, average rotational energy per molecule e_R, average vibrational-rotational energy per molecule e_{vR}, and average vibrational-rotational energy removed in a dissociation ε (rotationless model).

inversion seems to be the dominant phenomenon. The inversion in this rotationless model seems to spread from higher levels to the lower levels in time. As in the heating case, the vibrational temperatures $T_v(1)$, $T_v(8)$ and $T_v(14)$, and T_{ve} are compared with the Landau-Teller prediction for the rotational and rotationless cases in Figs. 9a and b, respectively. $T_v(8)$ and $T_v(14)$ agree very well with the Landau-Teller prediction for the rotational model. $T_v(1)$ and T_{ve} depict a strong overshoot and probably will take a long time to revert back to the equilibrium value. Prediction by the rotationless model is very poor. Since in a cooling environment the recombination rate is the dominant one, we will concentrate on this rate instead of the forward rate in this case. The recombi-

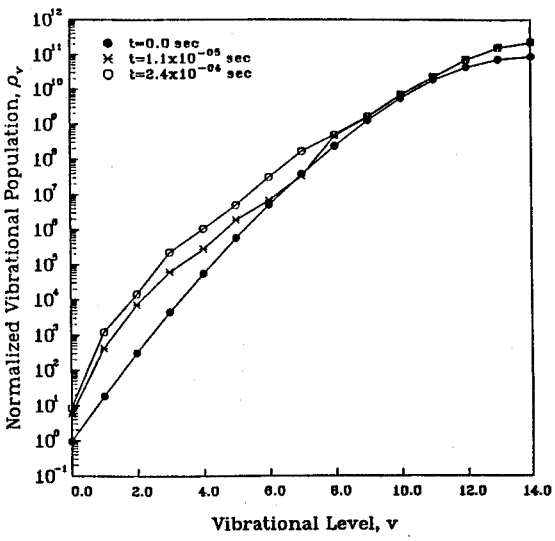

Fig. 7a Normalized vibrational population ρ_v as a function of the vibrational level, v, at selected times, in a cooling environment, T_0 = 2000 K → T = 1000 K (rotational model).

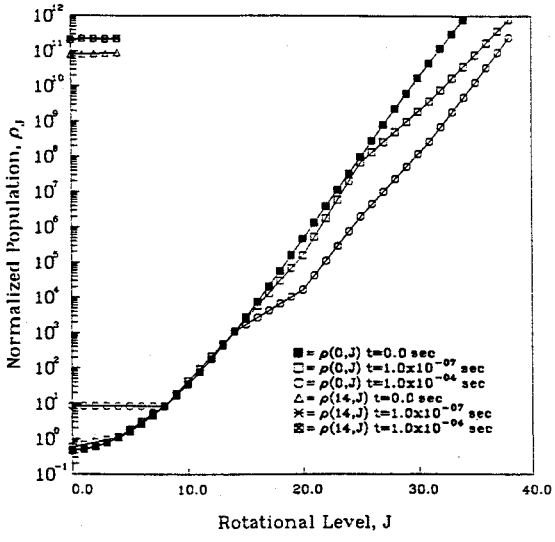

Fig. 7b Normalized rotational population ρ_J for v = 0 and 14 as a function of the vibrational level, v, at selected times, in a cooling environment, T_0 = 2000 K → T = 1000 K (rotational model).

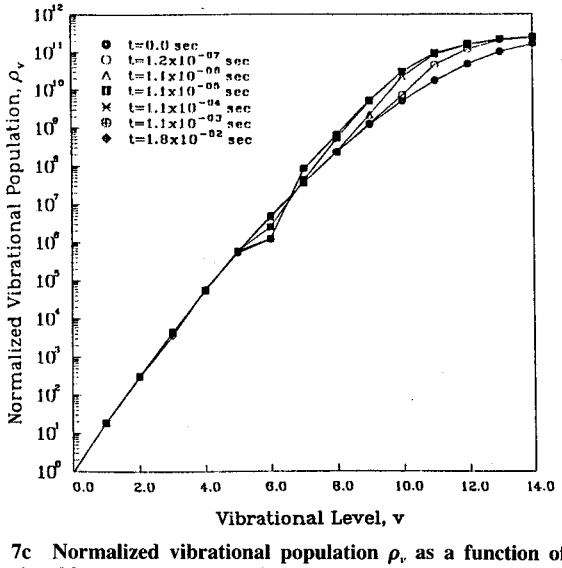

Fig. 7c Normalized vibrational population ρ_v as a function of the vibrational level, v, at selected times, in a cooling environment, T_0 = 2000 K → T = 1000 K (rotationless model).

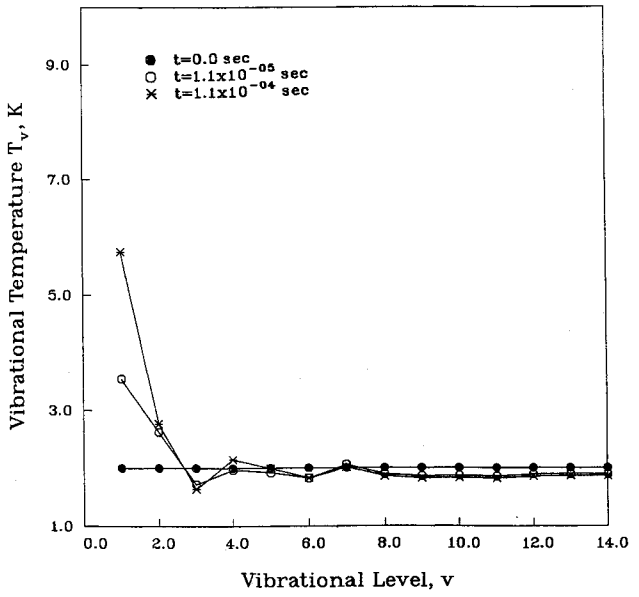

Fig. 8a Vibrational population expressed as vibrational temperature T_0 as a function of the vibrational level, v, at selected times, in a cooling environment, $T_0 = 2000$ K $\rightarrow T = 1000$ K (rotational model).

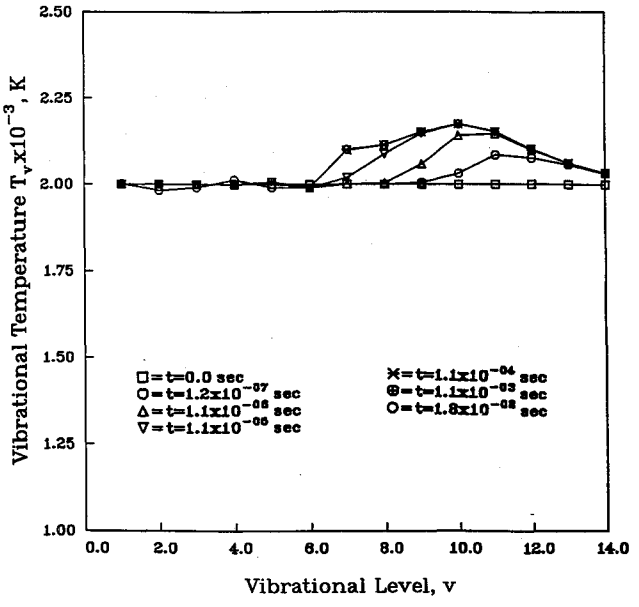

Fig. 8b Vibrational population expressed as vibrational temperature T_0 as a function of the vibrational level, v, at selected times, in a cooling environment, $T_0 = 2000$ K $\rightarrow T = 1000$ K (rotationless model).

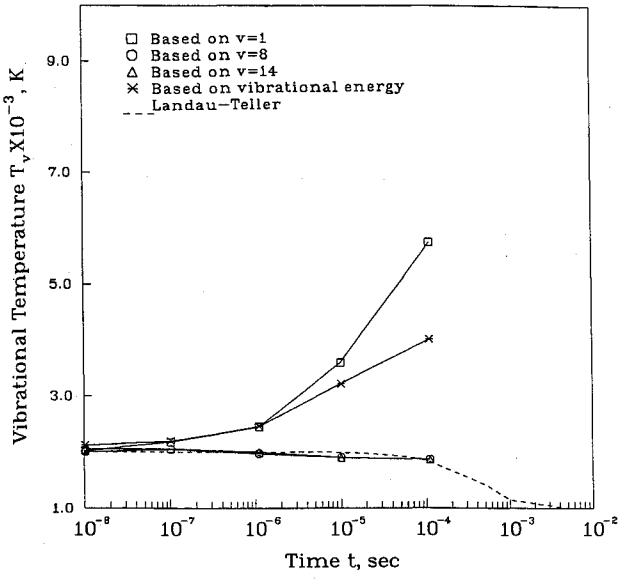

Fig. 9a Variation of the vibrational temperature based on v = 2, 8, and 14, and vibrational energy content, compared with the Landau-Teller prediction, in a cooling environment, $T_0 = 2000$ K $\rightarrow T = 1000$ K (rotational model).

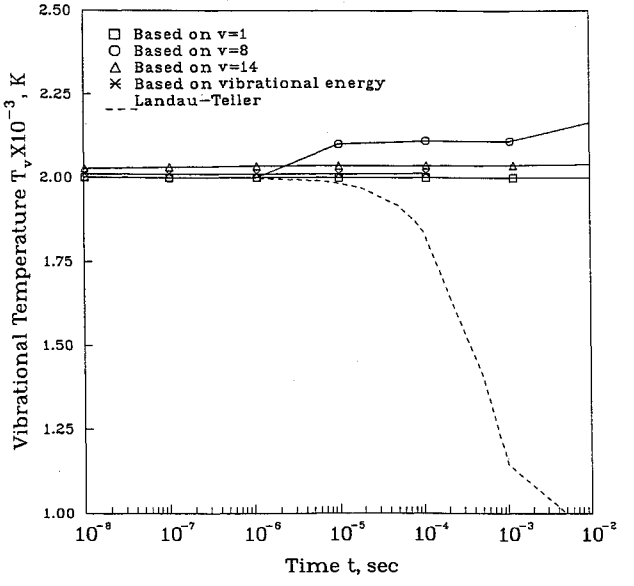

Fig. 9b Variation of the vibrational temperature based on v = 2, 8, and 14, and vibrational energy content, compared with the Landau-Teller prediction, in a cooling environment, $T_0 = 2000$ K $\rightarrow T = 1000$ K (rotationless model).

nation rates from the calculated solution, and from the empirical relationship[13]

$$K_r = 2.8 \times 10^{-31}\, T^{-0.6}\ \text{cm}^6/\text{s} \qquad (28)$$

by Cohen and Westberg, are plotted in Fig. 10 as a function of time.

The agreement between the value based on the present model and all the three other values computed using the Park model is good. A summary of the recombination rates from all exact calculations are plotted as a function of temperature in Fig. 11.

Also, comparison values obtained from Schwenke[5] and Cohen and Westberg[13] are also plotted in Fig. 11. The present rates are within one order of magnitude of the reported rates. The rotational model for $T = 1000$ K predicts $K_r = 8.6 \times 10^{-33}$ cm^6/s for the cooling case and $K_r = 2.0 \times 10^{-33}$ cm^6/s for the heating case. The rotationless model for $T = 1000$ K predicts $K_r = 1.2 \times 10^{-32}$ cm^6/s for the cooling case and $K_r = 1.29 \times 10^{-32}$ for the heating case.

Discussion

The results of this study, quantitatively, are similar to those as reported by Haug et al.[14] Haug solved a set of 162 rotational-vibrational master equations considering Ar-H_2 energy transfer and subsequent dissociation. Although, in Haug's study the disparity between the masses of the colliding partners was very large and there were no V-V energy transfers, the extent of nonequilibrium was found greater at higher vibrational and rotational levels.

The major difference between the results of the previous rotationless model[1] for N_2, and the results of the present rotational model for H_2 is that the minimum in the transition rate, $M(v)$, found in the former is not found in the latter. At high temperatures the average rotational quanta are large and the combined rotational-vibrational energy of the molecules

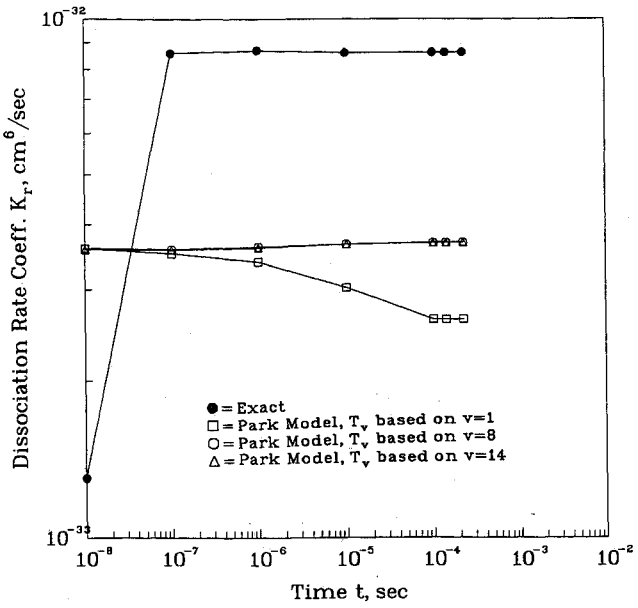

Fig. 10 The calculated recombination rate coefficient K_r compared with Park model, in a cooling environment, T_0 = 2000 K → T = 1000 K (rotational model).

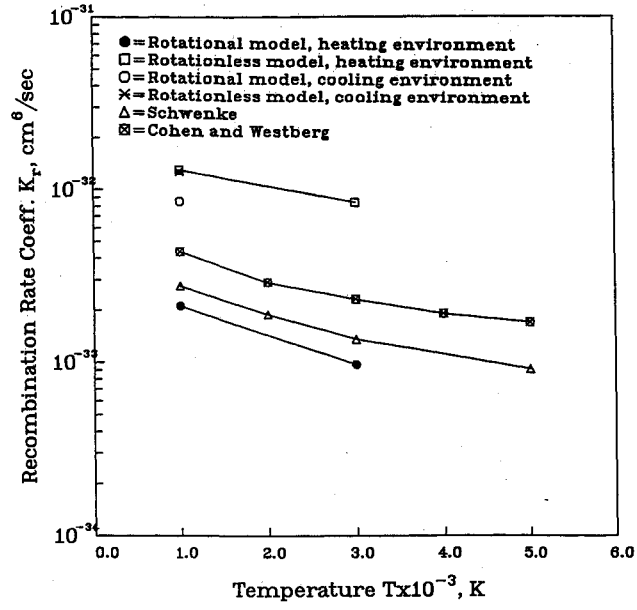

Fig. 11 The calculated recombination rates coefficients K_r as a function of temperature T.

at even lower vibrational levels cover a wide range, in small quantum jumps, with the ability to match with more than one vibrational-rotational quantum of the colliding partner, for a resonance energy transfer. The mid-levels, which were cutoff from the lower vibrational levels due to limited Δv in energy transfer, can now cause larger Δv. This way the mid-levels fully participate in the energy transfer and the minimum in the transition rate seen in the rotationless model does not appear in the rotational model.

During the relaxation, for both the cooling and heating environments, a fraction of the vibrational energy is transferred to the rotational states, near equilibrium, and it is transferred back to the vibrational states. This process seems to delay the dissociation process. In other words, one of the effects of the rotation is that the dissociation process is delayed. At higher rotational levels of lower vibrational levels, where the rotational energy constitutes a good fraction of the total internal energy, the molecule relaxes faster (see Figs. 3b and 7b). Overall effect of the rotation seems to be that it stretches the relaxation process a bit longer, very similar to Haug's results.[14]

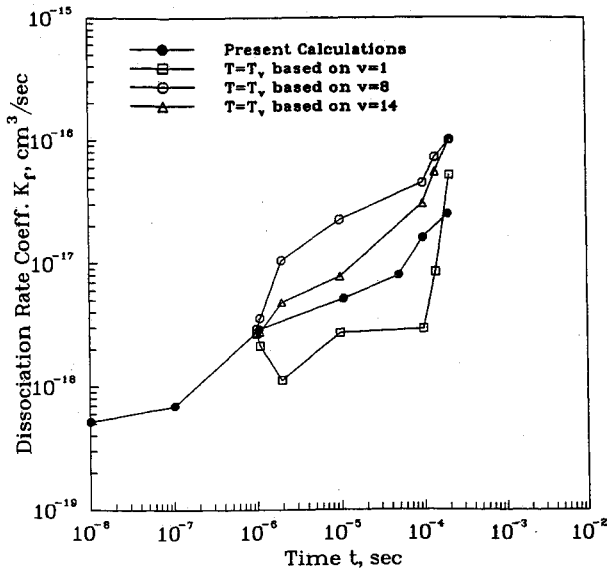

Fig. 12 The calculated recombination rate coefficient compared with the Park model, adjusted for 10^{-6} s incubation period, in a heating environment, T_0 = 2000 K → T = 3000 K (rotational model).

Experimental data reveal that the nonequilibrium relaxation of H_2 has a long incubation period. This incubation period is also evident in the present computations (see Figs. 2a and 4a). However, the empirical relationships, Eqs. (27) and (28), do not provide any clue to such an incubation period, since they are time independent as well as the rates computed in the present study. Therefore, it is not possible to compare the two rates without making some adjustment for this incubation period. For illustrative purposes, the dissociation rate data for the heating environment from Fig. 5a has been adjusted, assuming an incubation period of 10^{-6} s for the Park model data (The rates for the Park model were shifted ahead in time by 10^{-6} s), and plotted in Fig. 12. The agreement between the computed dissociation rate and the rates based on the empirical formulation and the Park model improves significantly by this adjustment.

For the heating environment, the dissociation rate and for the cooling environment, the recombination rate, agrees within one order of magnitude, when approximated using an empirical relationship from the equilibrium data with the temperature averaged using Park model. The accuracy can be improved if greater weight is given to T_v, such as $T_a = T^{0.3}T_v^{0.7}$. Since we have seen the rotational energy transfer plays an important role in the relaxation process of H_2 and in a two-temperature model, the vibrational temperature is the only parameter which accounts for the rotational-vibrational effects, it would be natural to put more weight on T_v.

In the rotational model of the heating case, the lower vibrational states get depressed (over-relax) severely, even below the equilibrium value, than predicted by the rotationless model. Similarly, in the cooling case, the lower states get inverted, above the equilibrium, more severely than predicted by the rotationless model. From the computations it seems that it would take a long time for these vibrational states to revert back to the equilibrium value. It is possible that the rotation of the molecules is in fact responsible for this behavior. It is also possible that since H_2 is the simplest molecule, and is highly quantized, that the quasi-classical trajectory theory does not provide satisfactory data for these first vibrational levels with low rotational energies. At this point no explanation is provided for this abnormal behavior.

The present work assumes that the vibrational transitions occur only through collisions with molecules. This assumption

is valid only when the degree of dissociation is low. When the degree of dissociation is significant, collisions with atoms contribute significantly to the overall transition rates. The rates of such transitions do not have the bottleneck phenomena seen in molecules. Therefore, most of the phenomena shown in the present work will be moderated by the presence of the atoms. Under those circumstances, the present work will exaggerate the effect of the molecule-molecule collisions in vibrational transitions.

Finally, detailed tests[15] show that the quasi-classical trajectory method is accurate for large transition probabilities, which is the case in the present study for the transition probabilities for $v \geq 4$. For $v = 0$, it is not clear how accurate the classical mechanics is. Comparison with experiments is not possible since no measurements of vibrational relaxation are available above 3000 K. So the accuracy of our calculations will have to be resolved by future work.

Conclusions

In the rotational model of H_2, the vibrational excitation rates do not have a minimum as was seen in the rotationless model of N_2. The mid-vibrational levels effectively participate in the relaxation process. However, they are not able to bridge the energy transfer gap between the lower and upper vibrational levels. The lower and upper vibrational levels seem to equilibrate to two different vibrational temperatures as in case of N_2. The rotation of the molecules helps in relaxing the molecule. During the relaxation a temporary transfer of energy from the vibrational degree of freedom to the rotational occur, which in effect delays the dissociation process and approach to equilibrium of the higher vibrational levels. Park's two temperature averaging technique can provide dissociation and recombination rates within one order of magnitude from equilibrium formulation of the rate data, provided the incubation period is properly accounted for. The average vibrational energy loss is about 80–90% of the dissociation energy.

References

[1]Sharma, S. P., Huo, W. M., and Park, C., "The Rate Parameters for Coupled Vibration-Dissociation in a Generalized SSH Approximation," AIAA Paper 88-2714, San Antonio, Texas, June 1988.

[2]Schwartz, R. N., Slawsky, Z. I., and Herzfeld, K. F., "Calculation of Vibrational Relaxation Times in Gases," *Journal of Chemical Physics*, Vol. 20, No. 10, 1952, pp. 1591–1599.

[3]Hammerling, P., Teare, J. D., and Kivel, B., "Theory of Radiation from Luminous Shock Waves in Nitrogen," *Physics of Fluids*, Vol. 2, No. 4, 1959, pp. 422–426.

[4]Treanor, C. E., and Marrone, P. V., "The Effect of Dissociation on the rate of Vibrational Relaxation," *Physics of Fluids*, Vol. 5, No. 9, 1962, pp. 1022–1026.

[5]Schwenke, D. W., "Calculation of Rate Constants for the Three-Body Recombination of H_2 in the Presence of H_2," *Journal of Chemical Physics*, Vol. 89, No. 4, 1988, p. 2076.

[6]Landau, L., and Teller, E., "Theory of Sound Dispersion," *Physikalische Zeitschrift der Sowjetunion*, Vol. 10, No. 34, 1936, pp. 34–43.

[7]Millikan, R. C., and White, D. R., "Systematics of Vibrational Relaxation," *Journal of Chemical Physics*, Vol. 39, No. 12, 1963, pp. 3209–3213.

[8]Park, C. "Two-Temperature Interpretation of Dissociation Rate Data for N_2 and O_2," AIAA Paper 88-0458, Reno, NV, Jan. 1988.

[9]Marrone, P. V., and Treanor, C. E., "Chemical Relaxation with Preferential Dissociation from Excited Vibrational Levels," *Physics of Fluids*, Vol. 6, No. 9, 1963, pp. 1215–1221.

[10]Truhlar, D. G., and Muckerman, J. T. "Reactive Scattering Cross Sections III: Quasi-Classical and Semi-Classical Method," *Atom-Molecule Collision Theory*, edited by Bernstein, R. B., Plenum, New York, 1979, p. 505.

[11]Bowen, S. W., "Spectroscopic and Optical Studies of a High Pressure, Under Expanded Jet," AIAA Paper 66-164, Monterey, CA 1966.

[12]Keck, J., and Carrier, G., "Diffusion Theory of Nonequilibrium Dissociation and Recombination," *Journal of Chemical Physics*, Vol. 43, No. 7, 1965, pp. 2284–2298.

[13]Cohen, N., and Westberg, K. R., "Chemical Kinetic Data Sheets for High-Temperature Chemical Reactions," *Journal of Physical Chemistry Reference Data*, Vol. 12, No. 3, 1983.

[14]Haug, K., and Truhlar, D. G., "Monte Carlo Trajectory and Master Equation Simulations of the Nonequilibrium Dissociation Rate Coefficient for $Ar + H_2 \rightarrow Ar + 2H$ at 4500 K," *Journal of Chemical Physics*, Vol. 86, No. 1, 1987, pp. 2697–2716.

[15]Duff, J. W., Blais, N. C., and Truhlar, "Monte Carlo Trajectory Study of $Ar + H_2$ Collisions: Thermally Averaged Vibrational Transition Rates at 4500 K," *Journal of Chemical Physics*, Vol. 71, No. 11, 1979, pp. 4304–4320.